

NOTICE: this is the author's version of a work that was accepted for publication in *Electrochimica Acta*. Changes resulting from the publishing process, such as peer review, editing, corrections, structural formatting, and other quality control mechanisms may not be reflected in this document. Changes may have been made to this work since it was submitted for publication. A definitive version was subsequently published in: *Electrochim. Acta* 55 (2010) 1450-1454. DOI: 10.1016/j.electacta.2009.05.008

New type of imidazole based salts designed specifically for lithium ion batteries

L. Niedzicki^{*,a}, G. Z. Żukowska^a, M. Bukowska^a, P. Szczeciński^a, S. Grugeon^{b,1},
S. Laruelle^{b,1}, M. Armand^{b,1}, S. Panero^{c,1}, B. Scrosati^{c,1}, M. Marcinek^{a,1}, W. Wieczorek^{a,1}

^a *Faculty of Chemistry, Warsaw University of Technology,
Noakowskiego 3, 00664 Warsaw, Poland*

^b *Laboratoire de Reactivite et de Chimie des Solides University de Picardie Jules Verne,
33 rue de Saint-Leu, 80039 Amiens, France*

^c *Department of Chemistry, The University of Rome "La Sapienza",
Piazzale Aldo Moro 5, 00185 Rome, Italy*

Abstract

In this manuscript we announce new type of “tailored” imidazole-derived salts designed, synthesized and tested for application in lithium conductive electrolytes. Basic characterization of the structure of described materials has been made by Raman, IR and NMR (¹³CNMR, ¹⁹FNMR) techniques. DSC and CV studies showed thermal stability of all salts over 200°C and electrochemical stability in liquid and solid polymer solvents up to +4.6 V vs. metallic lithium anode and Al collectors. Such properties proved applicability of these salts as lithium electrolytes for modern types of lithium-ion batteries.

Keywords: Lithium-ion; Batteries; Salts; Electrolytes; Synthesis.

* Corresponding author. Tel.: +48 22 234 7421; fax: +48 22 628 2741
E-mail address: asalm@ch.pw.edu.pl (L. Niedzicki)

¹ ISE member

1. Introduction

For the last 20 years lithium batteries have been proven to be the most successful type of the energy storage so far. It is also the field of the fastest development in energy storage nowadays. Surprisingly, while there is a numerous list of publications on the new lithium cell electrodes materials (or additions to ones), with also big amount of those on electrolytes additives, there have been very little stress given to new salts used in lithium electrolytes themselves. Even though there have been some previous achievements in the field since the introduction of LiPF_6 in 1990's, in fact, no other salts made it through to commercial rechargeable battery cells [1].

Apart from those known before 1990 (LiClO_4 , LiAsF_6 , LiPF_6 , LiBF_4 or LiCF_3SO_3), so far there were very few promising introductions of new anions for lithium salts. Starting with LiTFSI ($\text{LiN}(\text{SO}_2\text{CF}_3)_2$) [2], then methide ones, $\text{LiC}(\text{SO}_2\text{CF}_3)_3$ [3], $\text{LiC}(\text{SO}_2\text{CF}_3)_2(\text{RCO})$ [4] and $\text{LiN}(\text{SO}_2\text{C}_2\text{F}_5)_2$ (LiBETI) [5]. Unfortunately, all of them including LiTFSI , LiBETI and methide anion salts had the crippling drawback of being unable to form a passivation layer on Al current collectors [6] when applied to a cell. $\text{LiN}(\text{SO}_2\text{CF}_3)_2$ and $\text{LiC}(\text{SO}_2\text{CF}_3)_3$ were also claimed to be too expensive for commercial application.

A whole new class of orthoborate chelate-type anions was introduced by Barthel and co-workers, e.g. lithium bis[1,2-benzenediolato(2-)-O,O']borate (LBBB) [7-9], than Xu and co-workers brought-in borates of lithium bis(oxalate)borate (LiBOB) type and other chelate ones [10, 11]. While chelate salts based systems suffered from high viscosity (because of bulkiness of the anion) and as a result, poor conductivity, LiBOB and similar salts electrolyte systems were found to form poorly conducting solid electrolyte interface, which led to low power battery capability. These salts exhibit also poor solubility in commercial-type solvents and, thus, the electrolytes obtained exhibited weaker conductivity [6, 10]. The best of this class was lithium tetrakis(haloacyloxy)borates family (LiTFAB) introduced by Yamaguchi and co-workers [12], also suffering from low conductivity in the liquid electrolytes (much lower than LiTFSI or LiPF_6).

Other approach was to introduce phosphate salts – $\text{LiPF}_3(\text{CF}_2\text{CF}_3)_3$ (LiFAP) [13] or lithium tris[1,2-benediolato(2-)-O,O']phosphate [14]. Unfortunately, the first one is too expensive to be applied in commercial cells and the other lacked high conductivity in liquid solvents - again due to the high viscosity of the obtained electrolyte caused by the large anion size.

Also a few other ideas appeared along the years, such as using BF_3 compound as an electron-withdrawing group in, among the others, imidazole anions [15]. Low

conductivity (much lower than LiPF_6) of such salts applied as the electrolytes is the main drawback of this approach. The idea of application of sulfonyl fluorides (like $\text{ArS}(\text{CF}_2)_n\text{SO}_3\text{Li}$) as the new salts for electrolyte systems was also presented [16]. So far the only existing conductivity data have shown the results only slightly better than for LiTf (LiCF_3SO_3) [17].

After almost 20 years of applications of lithium cells there is still a lack of potential substitutes for LiPF_6 , which is definitely not flawless. Among the most important drawbacks of the LiPF_6 use in electrolyte system is the formation of HF. Hydrogen fluoride is the corrosive product of LiPF_6 slow decomposition (most probably through the hydrolysis with trace moisture [18]) in the cell, which destroys the cell from inside after certain time. With this on mind, new “tailored” anions especially for application as lithium electrolytes have been designed and investigated here.

Following salts have been synthesized and characterized: lithium 4,5-dicyano-2-(trifluoromethyl)imidazole (working name LiTDI), lithium 4,5-dicyano-2-(pentafluoroethyl)imidazole (LiPDI) and lithium 4,5-dicyano-2-(n-heptafluoropropyl)imidazole (LiHDI).

Main idea was to design structure that would not have disadvantages of big bulky anions causing high viscosity when dissolved in organic solvents, therefore a decrease in conductivity. Also, ions of new salts should not form agglomerates after dissolution, due to ion pairs' and triplet's negative effect on conductivity of an electrolyte, mechanism of lithium cations insertion into the electrodes (in both charging and discharging process) and transference number of a lithium cation. The last one causes the decrease of the energy storage reliability (energy put against energy retrieved).

Newly designed imidazole derivatives seem to perfectly fit into this scheme. These new salts were synthesized, using the procedure previously described[19] by our group. In the following section synthesis of salts and their basic characteristics will be described.

2. Experimental

2.1. Experimental techniques

Nuclear magnetic resonance (NMR) spectra were recorded on Varian Gemini 200. ^{13}C chemical shifts are reported relative to CD_3CN ($\delta = 1.3$). The ^{19}F shifts are described with CFCl_3 as the reference ($\delta = 0$).

Raman spectra were obtained on Nicolet Almega spectrometer. Diode lasers with excitation line 532 nm (for LiTDI and LiHDI) and 780 nm (LiPDI) were used. The spectral resolution was about 2 cm^{-1} for all experiments.

Fourier transform infra-red (FT-IR) spectra were collected on Perkin Elmer System 2000 spectrometer, for samples dispersed in KBr discs. The resolution was equal to 1 cm^{-1} .

Differential scanning calorimetry (DSC) measurements were made on TA 200 calorimeter with modulation function. Heating rate was equal to $2\text{K}\cdot\text{min}^{-1}$.

Cyclic voltammetry (CV) and conductance measurements were performed on VMP3 multichannel potentiostat. Propylene carbonate (PC) samples were cycled in Li / electrolyte / SS (stainless steel) system and poly(ethylene oxide) (PEO) samples were measured in Li / electrolyte / MCMB (mesocarbon-microbeads) system. CV of PEO samples was performed in 90°C and CV of PC samples was performed in ambient temperature. CV scan rate of PEO samples was $0.1\text{ mV}\cdot\text{s}^{-1}$ and PC samples scan rate was $5\text{ mV}\cdot\text{s}^{-1}$.

2.2. Sample preparation

All samples for cyclic voltammetry were assembled in argon-filled drybox with moisture level less than 3ppm. Prior to assembly, poly(ethylene oxide) was vacuum-dried for 24 hours and propylene carbonate used was anhydrous (water level $>10\text{ppm}$). Salts were vacuum-dried for at least 4 hours in 130°C .

Samples of salts for DSC were vacuum-dried for 4 hours in 130°C .

2.3. Synthesis

Synthesis scheme for all salts mentioned above is presented on Fig. 1.

2.3.1. Chemicals used

1,4-Dioxane, anhydrous, 99.8%, Aldrich;

Acetonitrile, anhydrous 99.8%, Aldrich;

Diethyl ether, $>99.5\%$, POCh;

Benzene, $>99.5\%$, POCh;

Diaminomaleonitrile, 98%, Aldrich;

Lithium carbonate, 99%, POCh;

Trifluoroacetic anhydride, $>99\%$, Sigma-Aldrich;

Pentafluoropropionic anhydride, derivatization grade 99%, Aldrich;

Heptafluorobutyric anhydride, derivatization grade, Aldrich.

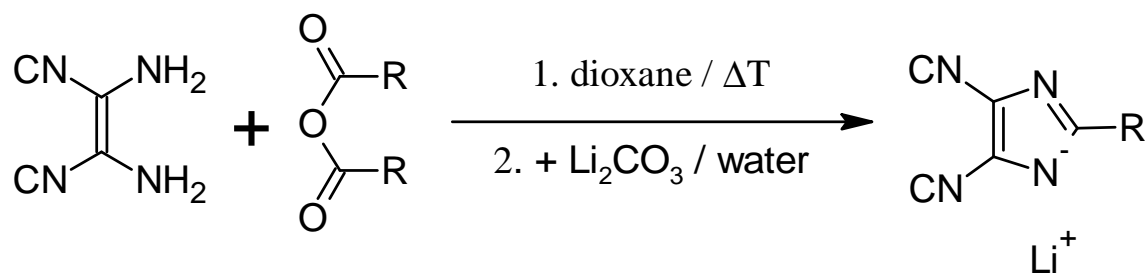


Fig. 1. Synthesis scheme for salts described in the text. $R = CF_3, C_2F_5, n-C_3F_7$.

2.3.2. Lithium 4,5-dicyano-2-(trifluoromethyl)imidazole

Trifluoroacetic anhydride (4.2 mL, 30 mmol) was poured into dicyanomaleonitrile solution (2.7 g, 25 mmol) in 1,4-dioxane (26 mL). Mixture was refluxed under argon atmosphere until the substrate disappeared (proved by TLC – Thin Layer Chromatography, after about 3h of heating). Resulting mixture was evaporated under vacuum (2 hours), where solvent and acid were removed. Solid residue was dissolved in diethyl ether (50 mL) and resulting solution was extracted three times with lithium carbonate (2.6g, 35 mmol) suspension in water (70 mL). Water solution of a salt was washed four times with ether (10 mL x 4). Then the decolorizing activated charcoal was added to water solution and the slurry was heated (2 hours, 45°C). After filtering off the charcoal on filter paper, the water was evaporated under vacuum (1 hour) and the resulting solid was dried on the vacuum line (1 hour, 90°C). Then the residue was dissolved in anhydrous acetonitrile and filtered of solid residue. The solvent was evaporated under vacuum (1 hour). Twice crystallization from 1:1 mixture of acetonitrile and benzene gives colorless crystals, which were put on the high vacuum drier line (4 hours, 120°C) giving lithium salt of 4,5-dicyano-2-(trifluoromethyl)imidazole (2.39 g, 50% yield). IR(KBr)/cm⁻¹ 2244 (CN stretching), 1501 (ring stretching), 1464 (ring stretching), 1189 (CF stretching), 1141, 1002; Raman(532nm)/cm⁻¹ 2265(vs, CN stretching), 1504 (vs, ring stretching), 1464, 1319 (vs, ring stretching), 1002, 183; ¹³C NMR (50 MHz, CD₃CN) $\delta = 115.6$ (s, -CN), 121.1 (q, J = 268 Hz, -CF₃), 120.6 (q, J = 1 Hz, C=C), 148.7 (q, J = 37 Hz, C-CF₃); ¹⁹F NMR (188 MHz, CD₃CN) $\delta = -63.1$ (s, -CF₃).

2.3.3. Lithium 4,5-dicyano-2-(pentafluoroethyl)imidazole

Pentafluoropropionic anhydride (10.5 mL, 53.8 mmol) was poured into dicyanomaleonitrile solution (4.84 g, 44.8 mmol) in 1,4-dioxane (47 mL). Mixture was refluxed under argon atmosphere until the substrate disappeared (proved by TLC, after

about 6h of heating). Resulting mixture was evaporated under vacuum (1 hour) and then put on the high vacuum drying line (1 hour, 120°C), where solvent and acid were removed. Solid residue was dissolved in diethyl ether (40 mL) and resulting solution was extracted three times with lithium carbonate (3g, 40.5 mmol) suspension in water (100 mL). Water solution of a salt was washed two times with ether (50 mL x 2). Then the decolorizing activated charcoal was added to water solution and the slurry was heated (1 hours, 45°C). After filtering off the charcoal on filter paper, the water was evaporated under vacuum (2 hours). Then the residue was dissolved in anhydrous acetonitrile and filtered of solid residue. The solvent was evaporated under vacuum (1 hour). Twice crystallization from 1:1 mixture of acetonitrile and benzene gives colorless crystals, which were put on the high vacuum drying line (4 hours, 120°C) giving lithium salt of 4,5-dicyano-2-(pentafluoroethyl)imidazole (5.12 g, 47.2% yield). IR(KBr)/cm⁻¹ 2260 (CN stretching), 1422 (ring stretching), 1340, 1212 (CF stretching), 1162 (CF stretching), 1053, 958; Raman(780nm)/cm⁻¹ 2267 (vs, CN stretching), 2261(vs, CN stretching), 1494(vs, ring stretching), 1316 (vs, ring stretching), 958, 540, 173; ¹³C NMR (50 MHz, CD₃CN) δ = 110.8 (t of q, J = 38 Hz and 250 Hz, -CF₃), 115.5 (s, -CN), 119.9 (q of t, J = 38 and 283 Hz, Im-CF₂-), 120.9 (t, J = 1 Hz, C=C), 147.5 (t, J = 26Hz, C-CF₂); ¹⁹F NMR (188 MHz, CD₃CN) δ = -83.1 (t of m, J = 1 Hz, -CF₃), -111.2 (q of m, J = 1 Hz, Im-CF₂-).

2.3.4. Lithium 4,5-dicyano-2-(n-heptafluoropropyl)imidazole

Heptafluorobutyric anhydride (14.9 mL, 60.83 mmol) was poured into diaminomaleonitrile solution (5.05 g, 46.79 mmol) in 1,4-dioxane (60 mL). Mixture was refluxed under argon atmosphere until the substrate disappeared (proved by TLC, after about 10h of heating). Resulting mixture was evaporated in the vacuum (1.5 hours) and further dried on the high vacuum drying line (4 hours, 140°C), where solvent and acid were removed. Solid residue was dissolved in diethyl ether (100 mL) and resulting solution was extracted three times with lithium carbonate (3.48g, 47 mmol) suspension in water (450 mL). Water solution of a salt was washed three times with ether (100 mL x 3). Then the decolorizing activated charcoal was added to water solution and the slurry was heated (1 hour, 45°C). After filtering off the charcoal on filter paper, the water was evaporated under vacuum (2 hours, 70°C). Then the residue was dissolved in anhydrous acetonitrile and filtered of the solid residue. The solvent was evaporated under vacuum (2 hours). Crystallization from 1:1 mixture of acetonitrile and benzene gives colorless crystals, which were put on the high vacuum drier line (4 hours, 140°C) giving lithium salt of 4,5-dicyano-2-(heptafluoropropyl)imidazole

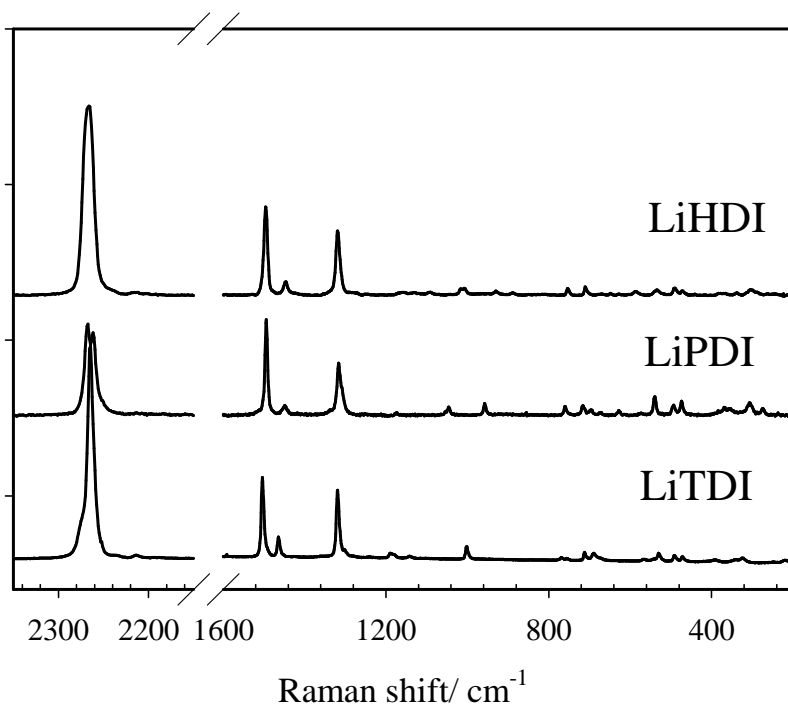


Fig. 2. Raman spectra of crystalline lithium 4,5-dicyano-2-(trifluoromethyl)imidazole (LiTDI), lithium 4,5-dicyano-2-(trifluoromethyl)imidazole (LiPDI), and lithium 4,5-dicyano-2-(n-heptafluoropropyl)imidazole (LiHDI).

(1.9 g, 13.9% yield). IR(KBr)/ cm^{-1} 2265 (CN stretching), 1672, 1220 (CF stretching), 1115 (CF stretching), 930, 888; Raman(532nm)/ cm^{-1} 2266(vs, CN stretching), 1495(s, ring stretching), 1319(s, ring stretching), 1008, 144(s); ^{13}C NMR (50 MHz, CD_3CN) δ = 109.9 (t of q, J = 37 and 265 Hz, $-\text{CF}_2-$), 112.6 (t of t, J = 30 and 252 Hz, $\text{Im}-\text{CF}_2-$), 115.7 (s, $-\text{CN}$), 119.0 (q of t, J = 33 and 287 Hz, $-\text{CF}_3$), 121.1 (s, $\text{C}=\text{C}$), 147.6 (t, J = 27 Hz, $\text{C}-\text{CF}_2$); ^{19}F NMR (188 MHz, CD_3CN) δ = -80.1 (t, J = 4 Hz, $-\text{CF}_3$), -109.8 (q of t, J = 1 Hz and 4Hz, $\text{Im}-\text{CF}_2-$), -126.2 (m, $-\text{CF}_2-$);

3. Results and discussion

Raman spectra of all studied salts: LiTDI, LiPDI and LiHDI (Fig. 2) exhibit similarities which confirm their chemical structure. The strongest band, with maximum at 2264 cm^{-1} corresponds to CN stretching vibrations of nitrile groups, two other strong bands can be ascribed to ring stretching vibrations, namely $\text{C}=\text{C}$ stretching (at $\sim 1495\text{ cm}^{-1}$) and $\text{C}=\text{N}$ stretching (1318 cm^{-1}). It is worth to notice that peak of the $\text{C}\equiv\text{N}$ stretching mode is split in spectra of LiPDI and LiHDI. In spectrum of LiPDI two distinct maxima at 2268 and 2262 cm^{-1} can be seen, while for LiHDI we observed broadening and an asymmetry of this peak,

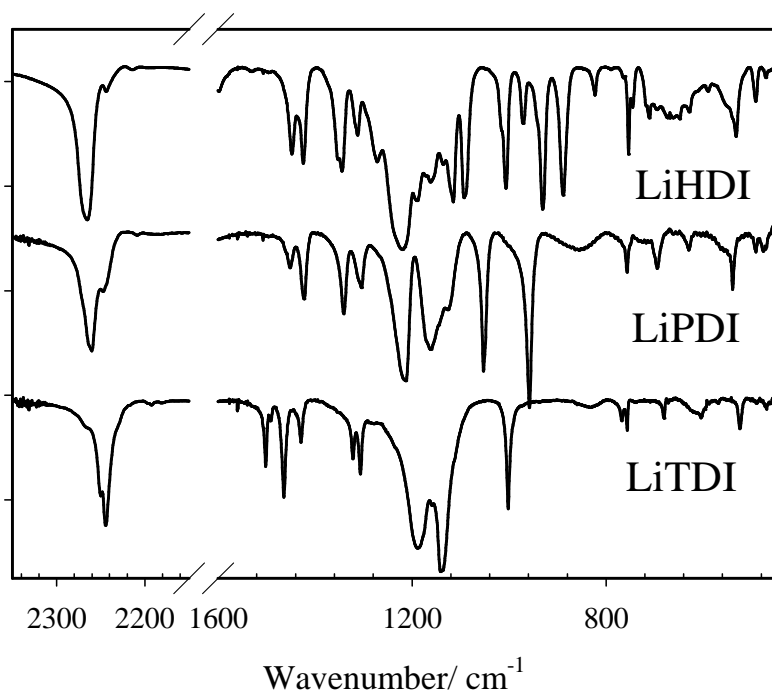


Fig. 3. FTIR spectra of imidazole derived salts in KBr - lithium 4,5-dicyano-2-(trifluoromethyl)imidazole (LiTDI), lithium 4,5-dicyano-2-(trifluoromethyl)imidazole (LiPDI), and lithium 4,5-dicyano-2-(n-heptafluoropropyl)imidazole (LiHDI).

which indicates that it must be a superposition of two highly overlapped bands. In spectrum of LiTDI the strong peak with maximum at 2264 cm^{-1} is accompanied by a weak shoulder at $\sim 2275\text{ cm}^{-1}$. Position of the main bands attributed to ring stretching vibrations is almost the same for LiPDI and LiHDI, while for LiTDI we observed of shift of peak attributed to C=C stretching vibration. We suspect that this effect is caused by the length of the side chain influencing the geometry of the compound. Difference between LiPDI and LiHDI on one hand and LiTDI on the other may result from higher flexibility of longer chain of substituent.

In FT-IR spectra (Fig. 3) a split of the ν_{CN} band is observed for all of these salts. In the spectral range of C \equiv N stretching vibration two bands can be distinguished, at approx. 2244 cm^{-1} and at 2260 cm^{-1} . The positions of maxima of the strongest peak in this spectral range is changing from 2244 cm^{-1} for LiTDI to 2260 and 2265 cm^{-1} for LiPDI and LiHDI, respectively. Additionally, both these bands exhibit further split: in LiTDI spectrum a second band at 2250 cm^{-1} is seen, while for LiPDI and LiHDI there is a shoulder on the higher wavenumbers of the main band.

Salt	T _r / K	T _m / K	ΔH / kJ·mol ⁻¹	T _{dec} (K)
LiTDI		433	80.23	480
LiPDI	447	498	72.64	504
LiHDI	409	481	78.34	486

Table 1. DSC data for LiTDI, LiPDI, LiHDI; T_r - max of the recrystallization signal, T_m - maximum of the melting peak, T_{dec} - onset of the decomposition.

Stability of the electrolyte is one of the key important properties in terms of applicability of these salts in the electrolyte. Thermal and electrochemical stability tests were performed for all three salts. Thermal stability was checked by DSC technique (Table 1). During heating, no thermal effect was observed before recrystallization process for LiPDI and LiHDI – 447 K (174°C) and 409 K (136°C), respectively. Interesting but logic there is no such a change in LiTDI (first analogue) having the shortest side chain. Maximum of the melting peak occurred, at 433 K (160°C,) for LiTDI, 498 K (225°C) for LiPDI and 481 K (208°C), for LiHDI. Melting enthalpy, was just the reciprocal of melting point order, the lowest for the LiPDI, with LiHDI lower than for LiTDI, and was equal to 80.24 kJ / mol, 72.64 kJ / mol and 78.34 kJ / mol (for LiTDI, LiPDI and LiHDI, respectively) . The first signs of thermal decomposition appeared at thermograms at 480 K (207°C) for LiTDI, 504 K (231°C) for LiPDI and 488 K (215°C) for LiHDI. These values are more than enough for all of salts for use in batteries. Note that it is higher than any modern ionic or polymer lithium cell can operate – either because of solvents, membranes or electrode thermal stability.

Electrochemical stability was tested by cyclic voltammetry for solutions in propylene carbonate (PC) and poly(ethylene oxide) of average molecular weight of 5·10⁶ g/mol (PEO). Samples contained solutions of anhydrous PC and 0.5 mol/L of each type of salt have been prepared and placed between stainless steel/metallic lithium electrodes. Cyclic voltammograms are pictured on Fig. 4. As it can be seen, there is high stability of salts within range +0.5 to +4.0 V vs. Li anode. Upper bound is ranging for salts between +4.3 V (LiPDI) and +4.5 V (LiHDI). Around +0.5 V vs. Li starts PC decomposition, slight cathodic peak +1.0 V (and coupled anodic peak around +1.4 V) is connected with formation of Li-stainless steel alloy , and cathodic peak +1.4 V (and coupled with it anodic peak around +2.0 V) is connected with contaminations (like crystalline water) reduction. Shapes of peaks and their positions are consistent with those obtained for similar systems by Dautzenberg

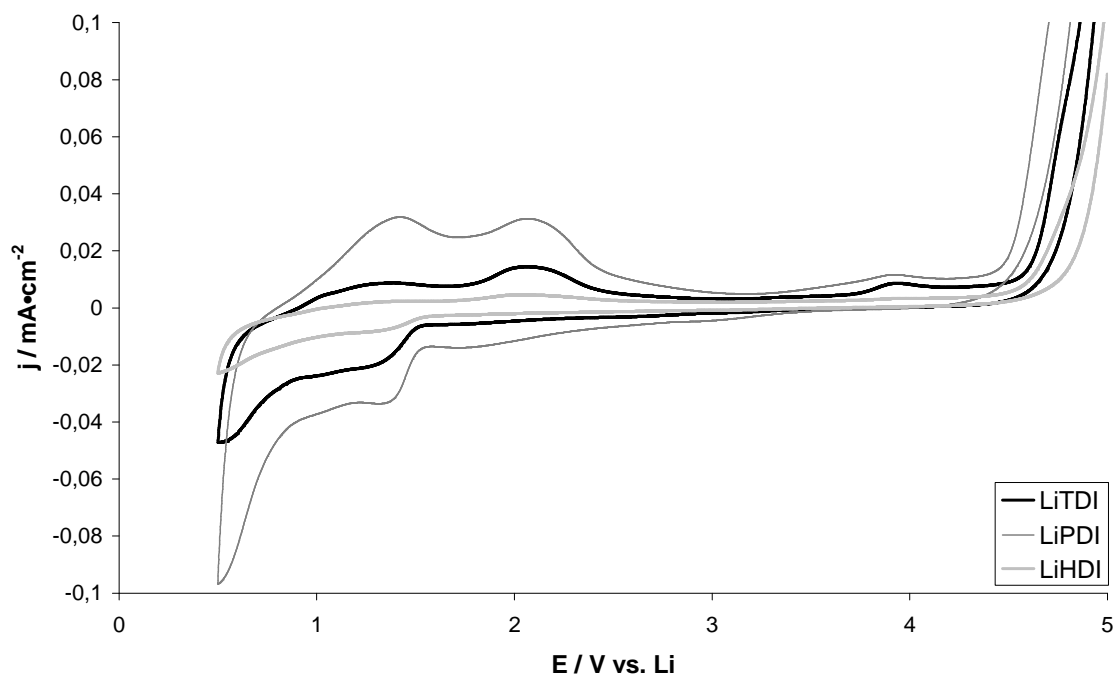


Fig. 4. Cyclic voltammeteries of 0.5M solutions of LiTDI, LiPDI and LiHDI in propylene carbonate with stainless steel blocking electrode as a working cell and lithium electrode as a counter electrode.

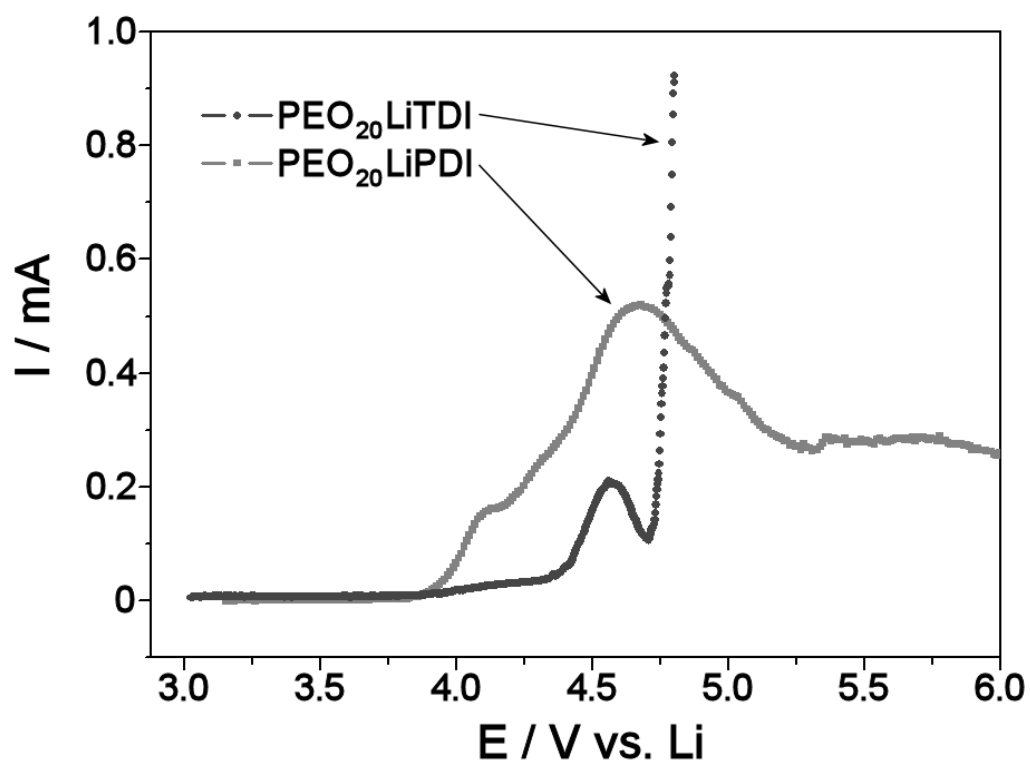


Fig. 5. Cyclic voltammeter of 1:20 Li/O ratio poly(ethylene oxide) (average molecular weight of $5 \cdot 10^6$ g/mol) membranes of LiTDI and LiPDI.

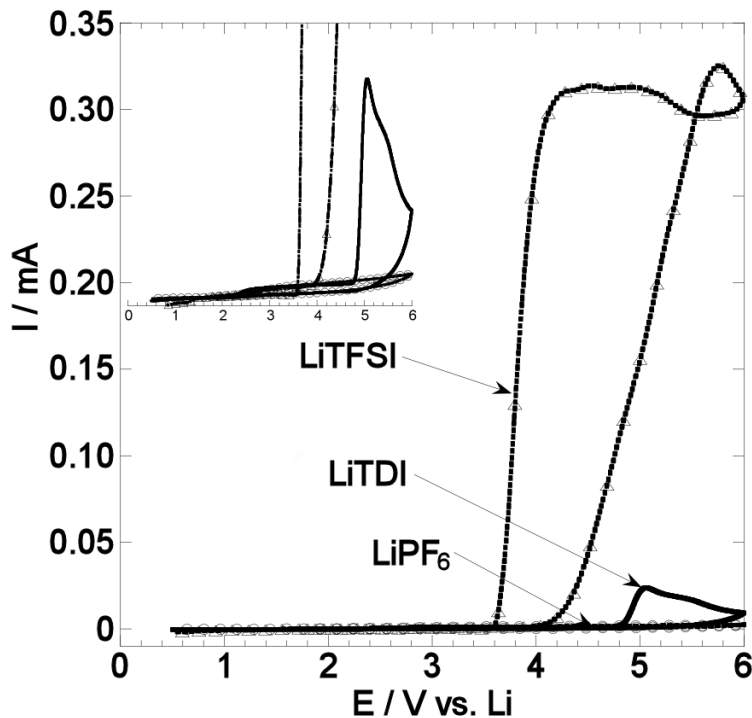


Fig. 6. Comparison of LiTDI stability against Al collectors with that of LiPF₆ and LiTFSI. There is a y-axis zoom of the graph in the top left corner of the figure.

et al. [20]. Stability up to +4.3 V for LiPDI is very good in the context of salts like LiBF₄, LiClO₄, which oxidize around +3.8 V, LiPF₆, which is stable up to +4.0 V [21] or other salts like LiAsF₆ or LiN(SO₂CF₃)₂ which have partial decompositions even around +2 V [20] (although LiN(SO₂CF₃)₂ is passivating electrode over time). It can be also pointed out that LiPDI has the highest current density during CV measurements.

For PEO linear voltammetry sweep, there membranes of 1:20 ratio of Li/O of LiTDI and LiPDI have been used. Results are shown on Fig. 5. Within range of -0.5 to 4.0 V there was no sign of any peaks, and at 4.0 V vs. Li anode there is a start of salt decompositions, which has been shown in details on the figure. That level of stability allows the salts to be used with all commercial types of cathodes, including LiFePO₄-type.

Finally, corrosiveness of a salt (LiTDI) against Al collectors has been checked. It was crucial for applicability, while few previously presented salts (imide and methide ones) were not forming stabilizing passive layer on Al. Result of the measurement is shown on Fig. 6, where LiTDI performance with Al is compared with other commonly known salts, namely LiTFSI and LiPF₆. LiTDI is having breakdown at 4.6 V, which is enough for application of this salt with all kinds of commercially used cathodes.

It is remarkable, that all data collected for all three salts show the tendency to be the highest (or the lowest) for LiPDI, with LiHDI for second place (like in melting and decomposition temperature, melting enthalpy) and LiTDI as the last (with stability against Li anode ex equo with LiHDI, and higher density current than LiHDI). We explain that as the compromise between the electron withdrawing group strength increase and its influence on whole anion symmetry, where three carbon chain will start to bend on one side, while one and two carbon groups will be symmetrical. That is possibly why LiPDI can possess highest values for electrolyte parameters.

We also made an investigation into conductivity, lithium cation transference numbers and association of new salts applied in liquid polymer electrolytes. Ionic conductivity of such systems were in the 10^{-3} to 10^{-4} S·cm⁻¹ range for 1M-0.1M poly(ethylene glycol) solutions (PEG) in room temperature, transference numbers exceeded 0.5 for 0.1M PEG solutions and the association degrees were much smaller than for other lithium salts. Detailed description and complete data on these studies will be presented elsewhere.

4. Conclusions

In the present study, we have presented data on synthesis and basic physical properties of completely new lithium salts “tailored” for application as electrolytes in lithium and lithium ion batteries. One of the benefits is the simplicity of the synthesis, easy, one-step, effective, made from quite simple and cheap substrates, giving high reaction yield (for two first salts). We have also presented all basic spectra data (IR, Raman and NMR) characterizing new substances. Then we have provided information on thermal and electrochemical stability, including cyclic voltammetry against Al (in terms of stability on batteries current collectors) and lithium anode, both in PEO and PC.

We described the tendencies of parameters’ changes between the salts and made an attempt to explain them in terms of the anion structure. It is very probable, that the symmetry of the anion in association with equalizing charge density along the anion is the key to increase parameters of electrolytes.

All collected data show high stability: +4.6 V vs. Li against aluminum collectors, +4.0 V vs. Li anode in PEO, with thermal stability for all salts over 200°C. All those results meet expectations for the applicability of the presented salts in lithium electrolytes for lithium cells.

Acknowledgements

This research was made in cooperation within and financially supported by Alistore Network of Excellence.

References

- [1] M. Winter, R. Brodd, *Chem. Rev.* 104 (2004) 4245.
- [2] F. Alloin, J. Y. Sanchez, M. B. Armand, *Electrochim. Acta* 37 (1992) 1729.
- [3] L. A. Dominey, V. R. Koch, T. J. Blakley, *Electrochim. Acta* 37 (1992) 1551.
- [4] D. Benrabah, J. Y. Sanchez, M. Armand, *Solid State Ionics* 60 (1993) 87.
- [5] L. J. Krause, W. Lamanna, J. Summerfield, M. Engle, G. Korba, R. Loch, R. Atanasoski, *J. Power Sources* 68 (1997) 320.
- [6] V. Aravindan, P. Vickraman, *Eur. Polym. J.* 43 (2007) 5121.
- [7] J. Barthel, R. Buestrich, E. Carl, H. J. Gores, *J. Electrochem. Soc.* 143 (1996) 3572.
- [8] J. Barthel, R. Buestrich, H. J. Gores, M. Schmidt, M. Wuhr, *J. Electrochem. Soc.* 144 (1997) 3866.
- [9] J. Barthel, M. Schmidt, H. J. Gores, *J. Electrochem. Soc.* 145 (1998) L17.
- [10] W. Xu, C. A. Angell, *Electrochem. Solid-State Lett.* 4 (2001) E1.
- [11] W. Xu, C. A. Angell, *Electrochem. Solid-State Lett.* 3 (2000) 366.
- [12] H. Yamaguchi, H. Takahashi, M. Kato, J. Arai, *J. Electrochem. Soc.* 150 (2003) A312.
- [13] M. Schmidt, U. Heider, A. Kuehner, R. Oesten, M. Jungnitz, N. Ignat'ev, P. Sartori, *J. Power Sources* 97-98 (2001) 557.
- [14] M. Handa, M. Suzuki, J. Suzuki, H. Kanematsu, Y. Sasaki, *Electrochem. Solid- State Lett.* 2 (1999) 60.
- [15] T. J. Barbarich, P. F. Driscoll, S. Izquierdo, L. N. Zakharov, C. D. Incarvito, A. L. Rheingold, *Inorg. Chem.* 43 (2004) 7764.
- [16] F. Toulgoat, B. R. Langlois, M. Medebielle, J.-Y. Sanchez, *J. Org. Chem.* 72 (2007) 9046.
- [17] E. Paillard, F. Toulgoat, J.-Y. Sanchez, M. Médebielle, C. Iojoiu, F. Alloin, B. Langlois, *Electrochim. Acta* 53 (2007) 1439.
- [18] K. Xu, *Chem. Rev.* 104 (2004) 4303.
- [19] M. Bukowska, J. Prejzner, P. Szczeciński, *Polish J. Chem.* 78 (2004) 417.
- [20] G. Dautzenberg, F. Croce, S. Passerini, B. Scrosati, *Chem. Mater.* 6 (1994) 538.
- [21] K. Kanamura, T. Umegaki, M. Ohashi, S. Toriyama, S. Shiraishi, Z. Takehara, *Electrochim. Acta* 47 (2001) 433.